Eur. Phys. J. A (2017) **53**: 162
DOI 10.1140/epja/i2017-12353-y

THE EUROPEAN PHYSICAL JOURNAL A

Special Article – Tools for Experiment and Theory

Prompt-delayed γ-ray spectroscopy with AGATA, EXOGAM and VAMOS++

Y.H. Kim[1,a], A. Lemasson[1,b], M. Rejmund[1], A. Navin[1], S. Biswas[2], C. Michelagnoli[1], I. Stefan[3], R. Banik[4], P. Bednarczyk[5], S. Bhattacharya[4], S. Bhattacharyya[4], E. Clément[1], H.L. Crawford[6], G. De France[1], P. Fallon[6], J. Goupil[1], B. Jacquot[1], H.J. Li[1], J. Ljungvall[7], A.O. Macchiavelli[6], A. Maj[5], L. Ménager[1], V. Morel[1], R. Palit[2], R.M. Pérez-Vidal[8], J. Ropert[1], and C. Schmitt[1]

[1] GANIL, CEA/DRF-CNRS/IN2P3, Bd Henri Becquerel, BP 55027, F-14076 Caen Cedex 5, France
[2] Department of Nuclear and Atomic Physics, Tata Institute of Fundamental Research, Mumbai 400005, India
[3] Institut de Physique Nucléaire, IN2P3-CNRS, Université Paris-Saclay, F-91406 Orsay Cedex, France
[4] Variable Energy Cyclotron Centre, 1/AF Bidhan Nagar, Kolkata 700064, India
[5] Institute of Nuclear Physics PAN, 31-342 Kraków, Poland
[6] Nuclear Science Division, Lawrence Berkeley National Laboratory, Berkeley, CA 94720, USA
[7] CSNSM, Université Paris-Saclay, CNRS/IN2P3, F-91405 Orsay, France
[8] IFIC, Universitat de València, CSIC, E-46071 València, Spain

Received: 19 May 2017 / Revised: 5 July 2017
Published online: 10 August 2017 –
Communicated by A. Gade

Abstract. A new experimental setup to measure prompt-delayed γ-ray coincidences from isotopically identified fission fragments, over a wide time range of 100 ns–200 μs, is presented. The fission fragments were isotopically identified, on an event-by-event basis, using the VAMOS++ large acceptance spectrometer. The prompt γ rays emitted at the target position and corresponding delayed γ rays emitted at the focal plane of the spectrometer were detected using, respectively, thirty two crystals of the AGATA γ-ray tracking array and seven EXOGAM HPGe Clover detectors. Fission fragments produced in fusion and transfer-induced fission reactions, using a ^{238}U beam at an energy of 6.2 MeV/u impinging on a ^{9}Be target, were used to characterize and qualify the performance of the detection system.

1 Introduction

The study of atomic nuclei in the phase space of large isospin, angular momentum and excitation energy, provides new insights to understand and predict the evolution of nuclear structure and the emergence of new phenomena in exotic nuclei [1,2]. Prompt and isomeric γ-ray spectroscopy of discrete states are powerful methods to achieve this goal. The occurrence of isomeric states in atomic nuclei is a manifestation of the underlying nuclear structure arising from specific collective or individual single-particle configurations of nucleons. The properties of isomeric states, their excitation energies, lifetimes and decay patterns, provide valuable constraints for understanding the structure of these nuclei [3,4]. Additionally, excitation modes built on isomers, observed through prompt γ-ray spectroscopy, can further help to characterize these specific structures. However, in the case of long-lived isomers ($t_{1/2} > 1\,\mu$s), it is challenging experimentally to correlate transitions feeding and depopulating the isomer and independent experimental setups are often required. Therefore, simultaneous measurement of correlations over a long time range for both prompt and delayed γ rays along with isotopic identification (Z, A), are critical to obtain unambiguous and complete level schemes.

Nuclear reactions at energies around the Coulomb barrier, such as fission [5,6] and multi-nucleon transfer [7,8] are powerful tools to populate neutron-rich exotic nuclei at large angular momentum. The recent combination of large acceptance spectrometers such as VAMOS++ [9,10] and PRISMA [11] with large arrays of Ge-detectors like EXOGAM [12], AGATA [13,14] or CLARA [15] has led to significant progress in the spectroscopy of exotic nuclei using prompt γ-ray spectroscopy [2,6,16–18]. The simultaneous measurement of the prompt, delayed and prompt-delayed γ rays of isotopically identified nuclei at energies around the Coulomb barrier will extend the experimental sensitivity and provide new insights into the evolution of nuclear structure far from stability.

A large experimental effort has been devoted to measure isomeric states in nuclei and an exhaustive discus-

[a] e-mail: yunghee.kim@ganil.fr
[b] e-mail: lemasson@ganil.fr

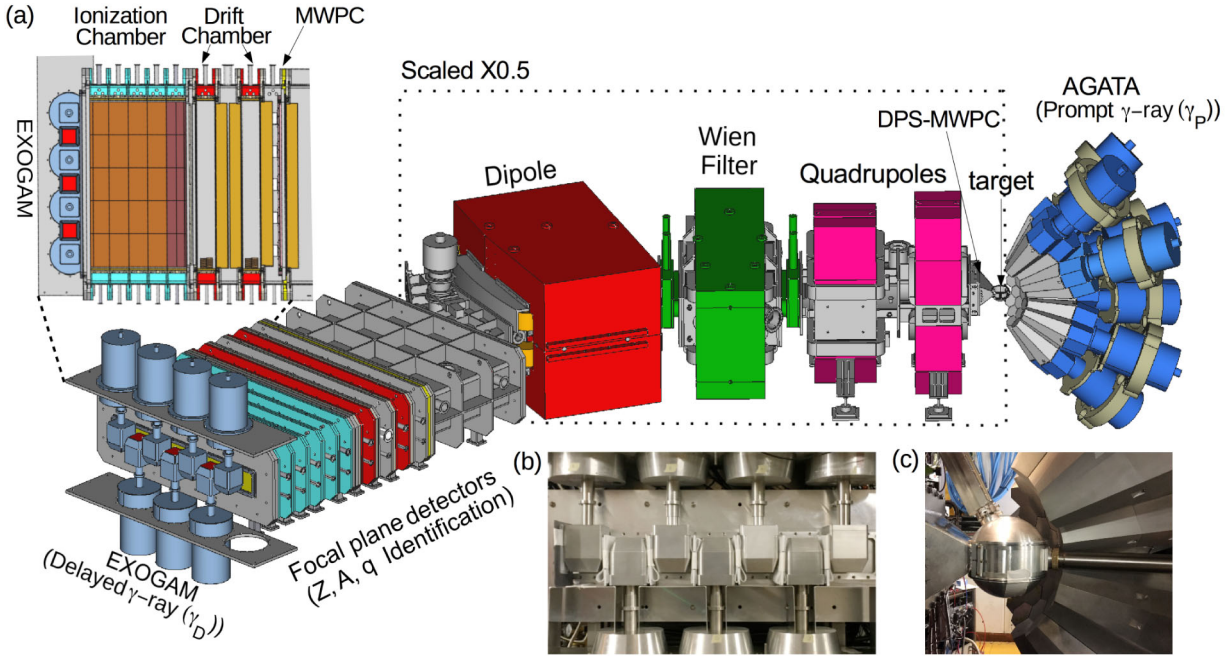

Fig. 1. (Color online) Experimental setup: (a) Top view of the focal plane detectors of VAMOS++ spectrometer and EXOGAM HPGe Clover detectors. (b) Picture of the EXOGAM HPGe Clover detectors at the VAMOS++ focal plane. (c) Picture of the target chamber and AGATA γ-ray tracking array.

sion of the various setups for isomer studies is presented in ref. [4]. These methods include delayed γ-ray spectroscopy coupled with isotopic identification from magnetic separator [19–21] or recoil decay-tagging [22] and prompt-delayed γ-ray correlations [23–28] using large γ-ray spectrometer array or recoil decay tagging [29]. However, it should be pointed out that prompt and delayed γ-ray correlation with simultaneous isotopic identification using a spectrometer was only reported for a limited number of cases such as ref. [30] and [31]. In this context, the present work reports on a new experimental setup, at GANIL, allowing a simultaneous measurement of prompt γ rays using AGATA and delayed γ rays using EXOGAM and their correlations, within a broad time range of 100 ns $\leq t_{1/2} \leq$ 200 μs, together with fission fragments isotopic identification obtained using the VAMOS++ spectrometer.

2 Experiment

The fission fragments were produced in fusion and transfer induced fission reactions using a ^{238}U beam at the energy of 6.2 MeV/u on a ^{9}Be target (1.6 and 5 μm thick) at GANIL. The typical beam intensities between 0.3 and 1 pnA were used. A schematic of the experimental setup is shown in fig. 1. Fission fragments were isotopically identified in (Z, A, q) using the VAMOS++ spectrometer [2, 9, 10], placed at 20° relative to the beam axis. The focal plane detection system of VAMOS++ consisted of a multi-wire proportional counter (MWPC) (time-of-flight), two drift chambers and a segmented ionization chamber $(\Delta E, E)$ having 6 rows (with a thickness of 5, 6, 12, 12, 12 and 10 cm) and 5 columns (with a width of 20.0 cm as shown in fig. 1). The ionization chamber was operated with CF_4 gas at 70 mbar. At the entrance of the spectrometer, the Dual Position-Sensitive MWPC [32] (DPS-MWPC) provided the start signal for the time-of-flight and the recoiling angle of the reaction products. The focal plane MWPC and drift chambers were operated with isobutane gas at 6 mbar. The fission fragments had a typical time-of-flight of 200 ns and were stopped in the ionization chamber (fig. 1(a)).

Prompt γ rays (γ_P) emitted at the target position by the recoiling reaction products were detected using the AGATA [14] γ-ray tracking array consisting of thirty two crystals (fig. 1(c)). To maximize the detection efficiency, the array was translated 10 cm towards the target compared to the nominal configuration, where the target is placed at the center of the array at 23.5 cm [33].

Delayed γ rays (γ_D) were detected using seven EXOGAM HPGe Clover detectors [12] arranged in a wall-like configuration at the focal plane of the VAMOS++ spectrometer (fig. 1(a) and (b)). A 2 mm thick aluminum window between the ionization chamber and the Clover detectors was used to minimize the attenuation of the emitted γ rays. A 3 mm thick lead shielding was placed after and in-between the Clover detectors to minimize the events arising from the room-background and Compton scattering between the Clover detectors. Typical off-beam background rates of EXOGAM were $\sim$ 550 Hz for each Clover detector with typical energy threshold of $\sim$ 60 keV. The typical in-beam rate was $\sim$ 750 Hz per Clover.

The event correlation between AGATA, VAMOS++ and EXOGAM was carried out using the time stamp

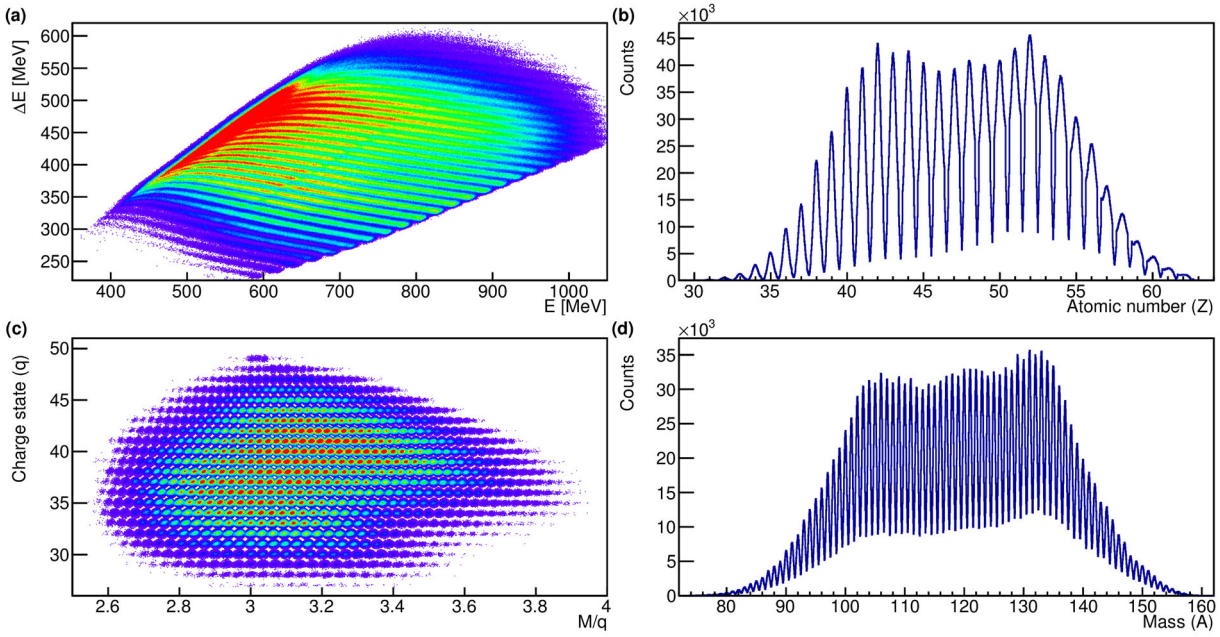

Fig. 2. (Color online) Particle identification spectra from the VAMOS++ spectrometer. (a) Energy loss (ΔE from the three first rows of the ionization chamber) *versus* total energy (E). (b) Atomic number (Z) obtained from the projection of the ΔE-E correlation matrix. (c) Charge state (q) *versus* mass over charge (M/q). (d) Reconstructed mass (A) (see text).

method with a clock frequency of 100 MHz. The prompt trigger was generated when both AGATA and VAMOS++ events were present within 300 ns. Typical singles trigger rates were ~ 7 kHz for the VAMOS++ and ~ 40 kHz for the AGATA array respectively. The delayed trigger for detecting delayed γ rays was generated when delayed γ-ray followed prompt trigger within 200 μs. The time between the ion implantation and the delayed γ-ray event was measured using time stamps difference.

3 Performance

3.1 Fission fragment identification

Event-by-event isotopic identification of fission fragments was obtained following a similar analysis procedure of the VAMOS++ spectrometer described in ref. [10]. In the present case, the total energy E was obtained from the sum of the energy deposited in all rows of the ionization chamber (while it was formerly measured in ionization chambers and the silicon wall). The atomic number was obtained from the two-dimensional spectrum ΔE-E shown in fig. 2(a), where ΔE was obtained from the sum of the first three rows of the ionization chamber and E from the sum of all rows. A typical Z spectrum, obtained from the projection on the Z lines is shown in fig. 2(b). The obtained resolution was $\Delta Z/Z = 1.3\%$ (FWHM) and represent an improvement compared to the previous setup described in ref. [10] (where $\Delta Z/Z = 1.5\%$). Figure 2(c) shows the two dimensional spectrum of charge state (q) *versus* mass over charge ratio (M/q) used to obtain mass identification and fig. 2(d) shows the resulting reconstructed mass (A). Typical resolutions of $\Delta q/q = 1.3\%$ (FWHM) and $\Delta A/A = 0.4\%$ (FWHM) were achieved.

3.2 γ-ray spectra

In the following section, we present the prompt and delayed γ-ray spectra of isotopically identified ^{132}Te and ^{94}Y. The well studied ^{132}Te [23, 34, 35] will be used to demonstrate the performance of this new setup. For completeness, the partial level scheme from ref. [23,34], up to an excitation energy of 4.3 MeV, is shown in fig. 3.

Prompt γ rays (γ_P)

The γ rays emitted in-flight were corrected for Doppler shift, on an event-by-event basis, using the velocity vector of the recoiling ions (measured by the DPS-MWPC detector) and the γ-ray emission angle (measured in AGATA). Gamma-ray interaction points were determined by the pulse shape analysis (PSA) using GRID search algorithm based on simulated pulse shape (AGATA data library) as described in ref. [36]. The interaction points were tracked using the Orsay Forward Tracking (OFT) algorithm [37] with standard input parameters to obtain the first interaction point and γ-ray emission angle for each of γ rays. The resolution of tracked Doppler corrected γ-ray energy was 5.0 keV (FWHM) for the $2^+ \rightarrow 0^+$ transition in ^{98}Zr at 1222.9 keV. The tracked Doppler corrected γ-ray energy resolution was limited by the γ-ray interaction point position resolution as discussed in ref. [32]. In the present

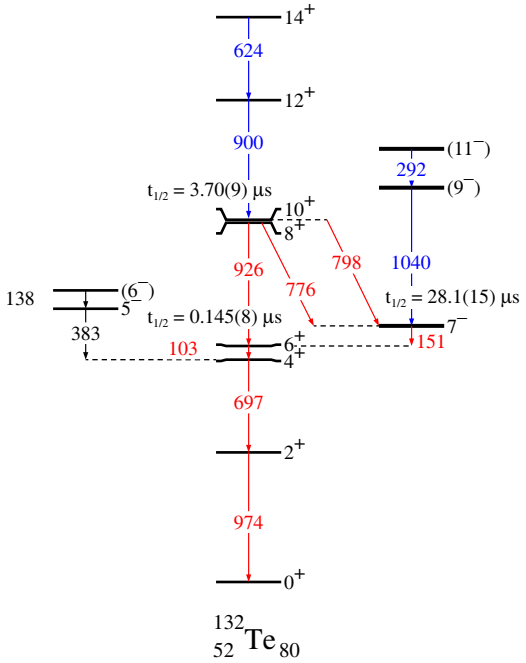

Fig. 3. (Color online) The partial level scheme of ^{132}Te (below 4.3 MeV). The transitions above (below) isomeric states are indicated in blue (red).

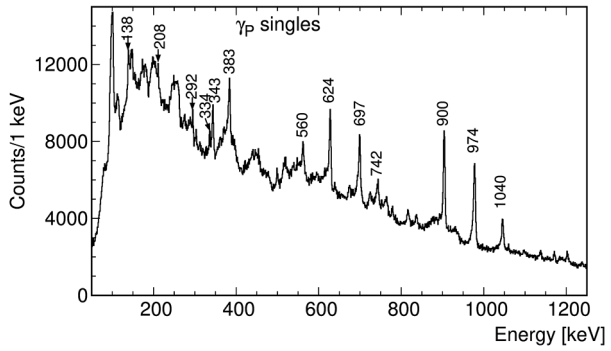

Fig. 4. Tracked Doppler corrected prompt γ-ray (γ_P) spectra for ^{132}Te "Singles" (Z, A) gated spectrum.

compact configuration, a γ-ray photo-peak efficiency (after tracking) of the AGATA of 9.5% at 1.2 MeV was measured using standard calibrated sources ^{152}Eu and ^{60}Co. Effect from the Lorentz boost at typical fragment velocity of $\beta = 0.1$ was simulated resulting in an in-beam tracked efficiency of 8.6% at 1.2 MeV.

The tracked Doppler corrected prompt γ-ray spectra (γ_P) measured in coincidence with isotopically identified ^{132}Te [23, 34] using AGATA detectors are presented in fig. 4. The γ-ray transitions depopulating states above the 10^+ isomeric state with $t_{1/2} = 3.7\,\mu$s ($E_{\gamma_P} = 208$, 334, 343, 560, 624, 742, 835, 900 keV), above the 7^- isomeric state with $t_{1/2} = 28\,\mu$s ($E_{\gamma_P} = 292$, 1040 keV), and the side band ($E_{\gamma_P} = 138$, 383 keV) can be seen. Also the transitions from the states below the isomers populated directly in fission were observed ($E_{\gamma_P} = 697$, 776, 974 keV). The broad peaks in fig. 4 are due to incorrect

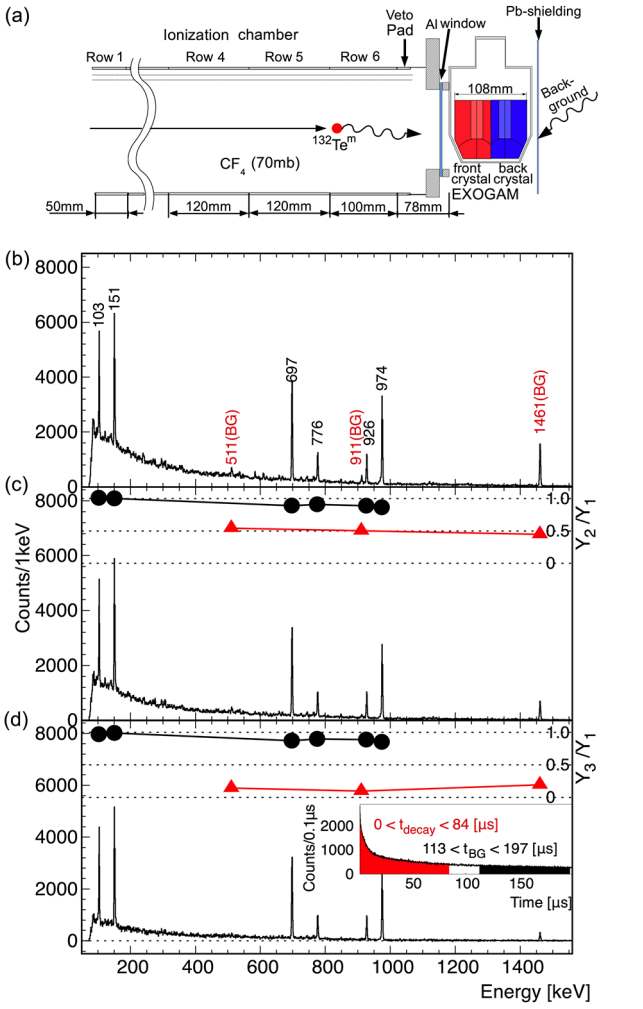

Fig. 5. (Color online) Delayed γ-ray spectra (γ_D) demonstrating the background reduction procedure: (a) A schematic side view of the ionization chamber and a single EXOGAM Clover. (b) In coincidence with ^{132}Te fragments for a time window of $0\,\mu\text{s} < t_{\text{decay}} < 84\,\mu$s. (c) Same as in (b) but with an additional condition that a front Ge-crystal was present in the event. The upper part of the figure shows the ratio of peak counts Y_2/Y_1 (with/without the condition). Filled circles (triangles) indicate the peaks belonging to ^{132}Te (room background). (d) Same as in (c) with background subtraction using the time stamp differences shown in the inset. The upper part of the figure illustrates ratio of peak counts Y_3/Y_1 (with all conditions/without condition) and the selected time windows obtained from the differences in time stamps.

Doppler correction of γ rays emitted from partner fission fragments. The appropriate Doppler correction for partner fission fragment can be carried out using kinematics calculation (*e.g.* see ref. [6, 38]).

Delayed γ rays (γ_D) and background reduction

Figure 5(a) shows the schematic side view of the ionization chamber and a single EXOGAM Clover detector. To recover events undergoing Compton scattering, the

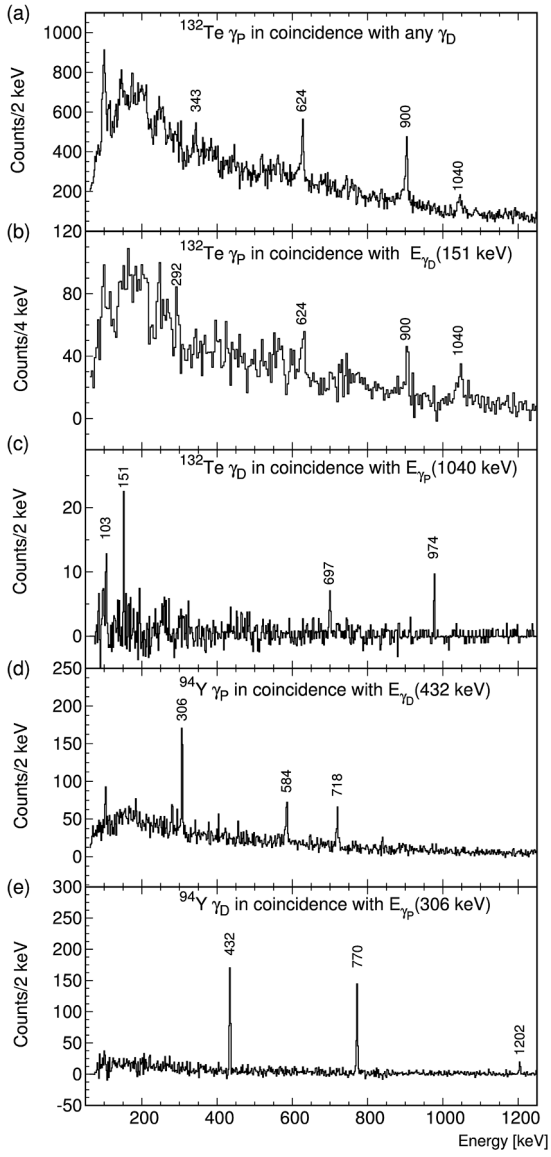

Fig. 6. Prompt-delayed coincidence spectra of ^{132}Te and ^{94}Y: (a) ^{132}Te Doppler corrected prompt γ-ray (γ_P) spectrum with the condition that a delayed γ-ray (γ_D) was detected, (b) Same as in (a) with the condition that a delayed γ-ray with energy $E_{\gamma_D} = 151\,\text{keV}$ was detected. (c) ^{132}Te delayed γ-ray (γ_D) spectrum in coincidence with prompt $E_{\gamma_P} = 1040\,\text{keV}$ γ-ray (d) ^{94}Y Doppler corrected prompt γ-ray (γ_P) with the condition that $E_{\gamma_D} = 432\,\text{keV}$ was detected. (e) ^{94}Y delayed γ-ray (γ_D) spectrum in coincidence with prompt $E_{\gamma_P} = 306\,\text{keV}$ γ-ray (see text).

measured signals from various crystals belonging to same Clover were added back. The delayed γ-ray (γ_D) spectrum obtained in coincidence with ^{132}Te identified by VAMOS++ in the time window $0\,\mu\text{s} < t_{\text{decay}} < 84\,\mu\text{s}$, is shown in fig. 5(b). The delayed γ rays (γ_D) belonging to ^{132}Te, transitions from the isomeric 10^+ state, $E_{\gamma_D} = 776$, 926 keV, and 7^-, $E_{\gamma_D} = 103$, 151, 697, 974 keV, can be identified. The transition $E_{\gamma_D} = 798\,\text{keV}$ is not intense enough to be visible and the $E_{\gamma_D} = 22\,\text{keV}$ ($10^+ \rightarrow 8^+$) is highly converted and below the experimental threshold. Gamma rays arising from the room background were observed as random coincidences and are labeled (BG). In the first step of the background suppression, it was required that a Ge-crystal facing the ion trajectory (red crystal in fig. 5(a)) was present in the event (*i.e.* events with γ rays hitting only the back crystals, shown as a blue crystal in fig. 5(a) were removed). The corresponding spectrum is shown in fig. 5(c). This condition reduced the room background by $\sim 50\%$ (see upper part of fig. 5(c)). In the subsequent step of the background suppression, the spectrum obtained in the time window $113\,\mu\text{s} < t_{\text{BG}} < 197\,\mu\text{s}$, normalized by the gate width, was subtracted (fig. 5(d)), reducing the room background to 20% (see inset in upper part of fig. 5(d)). This procedure preserved the area of γ-ray peak from ^{132}Te ($\sim 90\%$). Gamma-ray spectra shown later are treated with the background reduction procedure described above.

Prompt-delayed γ-ray correlation

The purpose of the present setup was to obtain the correlation between prompt and delayed γ rays along with an event-by-event isotopic identification of fission fragments. In fig. 6, prompt and delayed γ-ray spectra for isotopically identified ^{94}Y and ^{132}Te are shown to demonstrate the capabilities of the present setup. The Doppler corrected prompt γ-ray spectrum obtained in coincidence with any delayed γ-ray (γ_D) detected for the case of ^{132}Te is shown in fig. 6(a). Transitions from states placed below the isomeric states are not observed. Figure 6(b) shows the Doppler corrected prompt γ-ray spectrum obtained in coincidence with the delayed $E_{\gamma_D} = 151\,\text{keV}$. The transitions feeding both isomers are observed as they are interconnected [34]. The delayed γ-ray (γ_D) spectrum obtained in coincidence with prompt $E_{\gamma_P} = 1040\,\text{keV}$ transition feeding the 7^- state isomer (fig. 6(c)) shows only the γ rays from states below the 7^- isomeric state. Similar analysis in the case of ^{94}Y was also preformed and prompt (delayed) γ-ray spectra in coincidence with delayed (prompt) γ rays are show in fig. 6(d) and (e), respectively. The known delayed transitions (432, 770 and 1202 keV) depopulating the known isomeric state at 1202.4 keV reported in ref. [39] are observed. In addition prompt γ-ray transitions are observed in coincidence with the delayed γ-ray transition at 432 keV (fig. 6(d) and (e)). These transitions at 306, 584 and 718 keV are in agreement with recently reported levels in ^{94}Y [40,41].

3.3 Delayed γ-ray detection efficiency

The detection efficiency of the delayed γ-ray setup strongly depends on the penetration depth of the ions stopping in the ionization chambers and is thus to be determined case by case. Specific efficiencies can be extracted by gating on the prompt transitions feeding the isomeric state. The efficiency (ϵ) can be deduced as follows:

$$\epsilon = \frac{Y_D(1+\kappa_{EC})}{R_{BR}} \frac{1}{Y_P}\,, \tag{1}$$

Table 1. Efficiencies of delayed γ rays measured below the isomeric transitions in ^{94}Y and ^{132}Te with prompt γ-ray gate on 306 and 900 keV, respectively (see text).

^{94}Y		^{132}Te	
E_{γ_D} (keV)	ϵ (%)	E_{γ_D} (keV)	ϵ (%)
		103	1.9 ± 0.2
		151	1.5 ± 0.1
432	1.8 ± 0.1		
		697	0.8 ± 0.1
770	1.3 ± 0.1	776	0.6 ± 0.1
		926	0.6 ± 0.1
		974	0.5 ± 0.1
1202	0.8 ± 0.1		

where Y_D is the number of the coincident delayed transitions, R_{BR} is the branching ratio [42], κ_{EC} is the internal conversion coefficient [43] and Y_P is the number of the prompt transitions feeding the isomer. Typical efficiencies for the case of ^{132}Te and ^{94}Y are summarized in table 1, the prompt transitions used for gating were 900 keV and 306 keV, respectively. The larger efficiency observed in lighter and faster ^{94}Y as compared to the heavier ^{132}Te is due to the difference in penetration depth. These results are consistent with expectation from the geometry of the setup. Based on the present detection efficiencies of prompt and delayed γ rays, a typical overall prompt-delayed γ-ray detection efficiency of the order of 10^{-3} is obtained for the present setup.

3.4 Half-life measurements

Half-lives measurement were also investigated in the present experimental setup. The half-lives measurement of isomers in ^{132}Te will be used to exemplify the analysis procedure and performances. The typical in-beam rate of EXOGAM during the experiment was 5.3 ± 0.5 kHz. In such a case, the probability that an uncorrelated γ-ray triggers the system before the genuine isomer's decay is detected, becomes significant. Two effects arising from the uncorrelated random coincidences influence the raw fitted half-life that deviates from its true value. The first effect is the time-dependent background distribution, a typical time distribution obtained by gating on background counts is presented in fig. 7(a). It shows an exponential distribution, characteristic of random start (ions) and stop (γ-ray), similar to that shown in ref. [49]. This background time distribution was reproduced using the simulation assuming the random rate of 5.0 kHz (using Poisson distribution). Therefore, the γ-ray background subtraction of the time distribution is necessary. The second effect is the wrong stop time arising from the random coincidences. For a given isomer, the probability of detecting

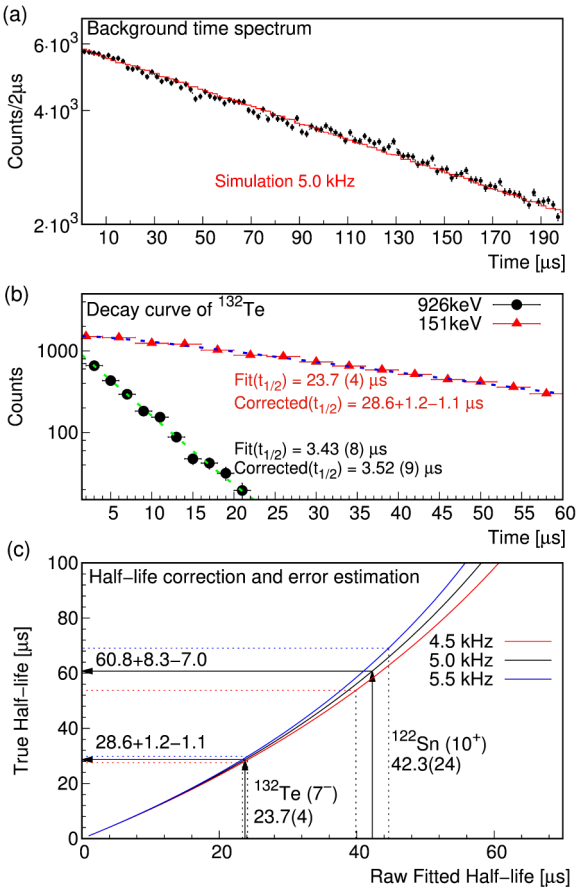

Fig. 7. (Color online) (a) Time distribution gated on γ-ray background (black filled circle) and simulated assuming the random γ-ray rate of 5.0 kHz (red solid line). (b) The background subtracted decay curve for the ^{132}Te isomeric transitions $E_{\gamma_D} = 151$ keV (filled red triangles) and the $E_{\gamma_D} = 926$ keV (filled black circles). The blue (green) dashed lines are the raw fitted two (single) component exponential curves corresponding to the 151 (926) keV transitions. The raw fitted half-life obtained from the fit along with the corrected true half-lives are given (see text). (c) The correlation between raw fitted half-life and true half-life for different random γ-ray rate of 5.0 kHz (black solid line), 4.5 kHz (red solid line) and 5.5 kHz (blue solid line). The raw fitted half-life of ^{132}Te 7^- ($23.7 \pm 0.4\,\mu$s) and ^{122}Sn 10^+ ($42.3 \pm 2.4\,\mu$s) is indicated by black solid/dotted vertical line and the corrected true half-life and the corresponding error accounting for the fluctuation of the rate is shown as a horizontal black solid and blue/red dotted line, respectively.

γ-ray from random background before the γ-ray depopulating isomer, within 200 μs coincidence gate increases as a function of half-life. This random coincidence results in a time distribution with fitted half-life shorter than its true value. The exemplified time distributions of the ^{132}Te, $E_{\gamma_D} = 151$ keV and the $E_{\gamma_D} = 926$ keV transitions with background subtraction are shown in fig. 7(b). The fit using Bateman equation to the $E_{\gamma_D} = 151$ keV time distri-

Table 2. Half-lives: Measured half-lives for the isomeric transitions in ^{94}Y, ^{122,124}Sn, ^{132,134}Te, and ^{136}Xe. A comparison with literature values is also shown.

Isomers	E_{γ_D} [keV]	I_{Isomer}	$I_i \rightarrow I_f$	$t_{1/2}$ [μs]	
				(This Exp.)	(Ref.)
^{94}Y	$770 + 432$	(5^+)	$(5^+) \rightarrow (3^-) \rightarrow 2^-$	1.33 ± 0.01	1.35 ± 0.02 [39]
^{122}Sn	281	(10^+)	$(8^+) \rightarrow (7^-)$	$60.8 + 8.3 - 7.0$	62 ± 3 [44]
^{124}Sn	120	(7^-)	$(7^-) \rightarrow (5^-)$	2.83 ± 0.12	3.1 ± 0.5 [45]
	253	(10^+)	$(8^+ \rightarrow 7^-)$	$55.0 + 4.7 - 4.1$	45 ± 5 [44]
^{132}Te	151	7^-	$7^- \rightarrow 6^+$	$28.6 + 1.2 - 1.1$	28.1 ± 1.5 [35]
	926	10^+	$8^+ \rightarrow 6^+$	3.52 ± 0.09	3.70 ± 0.09 [34]
					3.9 ± 0.3 [35]
^{134}Te	$115 + 297 + 1279$	6^+	$6^+ \rightarrow 4^+ \rightarrow 2^+ \rightarrow 0^+$	0.19 ± 0.01	0.197 ± 0.020 [46]
					0.165 ± 0.006 [47]
					0.164 ± 0.001 [48]
^{136}Xe	197	6^+	$6^+ \rightarrow 4^+$	2.92 ± 0.03	2.95 ± 0.09 [42]

bution, accounting for feeding from a shorter-lived 10^+ isomeric state, provides a raw fitted half-life of $23.7 \pm 0.4\,\mu$s. The fitted value is three sigma shorter than the literature value of $28.1 \pm 1.5\,\mu$s [35]. The fitted half-life of $E_{\gamma_D} = 926$ keV transition was $3.43 \pm 0.08\,\mu$s which is shorter but similar to the literature value $3.70 \pm 0.09\,\mu$s [34].

Simulation of decay time spectra was carried out to quantify the effect of the random coincidence on the half-life measurement, similar to that in ref. [49]. The result of the correlation between raw fitted half-life and true half-life, assuming random γ rates of 4.5, 5.0 and 5.5 kHz, is presented in fig. 7(c). The figure also shows the case of ^{132}Te 7^- and ^{122}Sn 10^+ isomers. The necessary correction of experimental half-life results in an increased uncertainty due to the instability of the experimental rate, which is of the order of 0.5 kHz. The effect from the random rate is significant for isomers with raw fitted half-life $\geq 30\,\mu$s causing more than $\sim 20\%$ correction in half-life with error ~ 3 times larger than the fitted value and illustrate the sensitivity of half-life to random rate in this type of experiment. The half-life of ^{132}Te 7^- and 10^+ isomer after the correction was $28.6 + 1.2 - 1.1\,\mu$s and $3.52 \pm 0.09\,\mu$s, respectively, which is in good agreement with the literature value [34,35] (see fig. 7(b)).

To further demonstrate the capabilities of the present experimental system, table 2 reports measured half-lives in various time ranges for different isotopes compared to the values given in the literature. The experimentally obtained half-lives are in good agreement with the literature values.

4 Summary and perspectives

A new experimental setup for prompt-delayed coincidence of isotopically identified fission fragments with isomeric states was presented. This setup consists of the unique combination of the AGATA and EXOGAM γ-ray detectors and the VAMOS++ large acceptance spectrometer. The performance of the system was studied using fission fragments produced in fusion and transfer induced fission reactions of a ^{238}U beam on a ^{9}Be target. Various types of γ-ion and γ-γ-ion coincidences were demonstrated including the measurements of half-life over a wide time range that are in agreement with the values reported in literature.

This powerful system at GANIL will be a unique tool to study nuclei produced from a variety of nuclear reactions around the Coulomb barrier with stable and radioactive ion beams (SPIRAL1 and SPIRAL2), compatible with the VAMOS++ detection system and its working modes. These include i) direct transfer reactions [50], ii) multi-nucleon transfer reactions [16], iii) fusion and transfer induced fission [2], iv) spontaneous fission v) fusion using VAMOS++ in the gas-filled mode [51].

In the near future, planned upgrades will further improve the sensitivity of the present system. First, dedicated digital electronics NUMEXO2 [52,53] for EXOGAM Clovers will be used for each crystal, providing individual time stamping and pileup treatment that will result in an improved data collection for long-lived isomers. Furthermore, the VAMOS++ detection system will benefit from digital electronics allowing a significant improvement of the data throughput and pileup treatment.

We would like to thank the AGATA Collaboration for the availability of the AGATA γ-ray tracking array at GANIL. We acknowledge the important technical contributions of the GANIL accelerator staff. PB and AM acknowledge support from National Science Centre under Contract No. 2013/08/M/ST2/00257 and the French LEA COPIGAL project. SB, RB, SB, SB and RP acknowledge support from the LIA France-India agreement. HLC, PF and AOM acknowledge support from the U.S. Department of Energy, Office of Science, Office of Nuclear Physics under Contract No. DE-AC02-05CH11231 (LBNL).

References

1. T. Otsuka, Phys. Scr. T **152**, 014007 (2013).
2. A. Navin *et al.*, Phys. Lett. B **728**, 136 (2014).
3. G.D. Dracoulis, Phys. Scr. T **152**, 014015 (2013).
4. J.A. Pinston, J. Genevey, J. Phys. G: Nucl. Part. Phys. **30**, R57 (2004).
5. S. Kailas, Phys. Rep. **284**, 381 (1997).
6. A. Navin, M. Rejmund, in *McGraw-Hill Yearbook of Science and Technology 2014* (McGraw-Hill, 2014) p. 137.
7. V. Volkov, Phys. Rep. **44**, 93 (1978).
8. L. Corradi, G. Pollarolo, S. Szilner, J. Phys. G: Nucl. Part. Phys. **36**, 113101 (2009).
9. S. Pullanhiotan *et al.*, Nucl. Instrum. Methods A **593**, 343 (2008).
10. M. Rejmund *et al.*, Nucl. Instrum. Methods A **646**, 184 (2011).
11. A. Stefanini *et al.*, Nucl. Phys. A **701**, 217 (2002).
12. J. Simpson *et al.*, Acta Phys. Hung. New Ser. Heavy Ion Phys. **11**, 159 (2000).
13. A. Gadea *et al.*, Nucl. Instrum. Methods A **654**, 88 (2011).
14. S. Akkoyun *et al.*, Nucl. Instrum. Methods A **668**, 26 (2012).
15. A. Gadea *et al.*, Eur. Phys. J. A **20**, 193 (2003).
16. Y.X. Watanabe *et al.*, Phys. Rev. Lett. **115**, 172503 (2015).
17. M. Rejmund *et al.*, Phys. Rev. C **93**, 024312 (2016).
18. M. Rejmund *et al.*, Phys. Lett. B **753**, 86 (2016).
19. J.A. Pinston *et al.*, Phys. Rev. C **61**, 024312 (2000).
20. P. Regan *et al.*, Nucl. Phys. A **787**, 491 (2007).
21. P.-A. Söderström *et al.*, Nucl. Instrum. Methods B **317**, 649 (2013) (Part B).
22. K. Hauschild *et al.*, Phys. Rev. Lett. **87**, 072501 (2001).
23. S. Biswas *et al.*, Phys. Rev. C **93**, 034324 (2016).
24. G. Bocchi *et al.*, Phys. Lett. B **760**, 273 (2016).
25. B. Fornal *et al.*, Phys. Rev. C **63**, 024322 (2001).
26. L.W. Iskra *et al.*, Phys. Rev. C **89**, 044324 (2014).
27. P. Bhattacharyya *et al.*, Phys. Rev. C **56**, R2363 (1997).
28. M. Houry *et al.*, Eur. Phys. J. A **6**, 43 (1999).
29. A. Hürstel *et al.*, Eur. Phys. J. A **15**, 329 (2002).
30. K. Wimmer *et al.*, Nucl. Instrum. Methods A **769**, 65 (2015).
31. A. Dijon *et al.*, Phys. Rev. C **85**, 031301 (2012).
32. M. Vandebrouck *et al.*, Nucl. Instrum. Methods A **812**, 112 (2016).
33. E. Clément *et al.*, Nucl. Instrum. Methods A **855**, 1 (2017).
34. J. Genevey *et al.*, Phys. Rev. C **63**, 054315 (2001).
35. K. Sistemich *et al.*, Z. Phys. A **292**, 145 (1979).
36. R. Venturelli, D. Bazzacco, LNL Annu. Rep. **2004**, 220 (2005).
37. A. Lopez-Martens *et al.*, Nucl. Instrum. Methods A **533**, 454 (2004).
38. A. Navin *et al.*, Phys. Lett. B **728**, 136 (2014).
39. J. Genevey *et al.*, Phys. Rev. C **59**, 82 (1999),
40. L. Iskra *et al.*, in *6th Workshop on Nuclear Fission and Spectroscopy of Neutron-Rich Nuclei (FISSION 2017)* (Chamrousse, France, 2017).
41. L. Iskra *et al.*, in preparation; private communication (2017).
42. ENSDF, `http://www.nndc.bnl.gov/ensdf/` (2017).
43. T. Kibédi *et al.*, Nucl. Instrum. Methods A **589**, 202 (2008).
44. R. Broda *et al.*, Phys. Rev. Lett. **68**, 1671 (1992).
45. B. Fogelberg, P. Carl, Nucl. Phys. A **323**, 205 (1979).
46. J.K. Hwang *et al.*, Phys. Rev. C **69**, 057301 (2004).
47. M. Mineva *et al.*, Eur. Phys. J. A **11**, 9 (2001).
48. J.P. Omtvedt *et al.*, Phys. Rev. Lett. **75**, 3090 (1995).
49. W. Urban *et al.*, Phys. Rev. C **79**, 044304 (2009).
50. B. Fernández-Domínguez *et al.*, Phys. Rev. C **84**, 011301 (2011).
51. C. Schmitt *et al.*, Nucl. Instrum. Methods A **621**, 558 (2010).
52. F.J. Egea *et al.*, in *2014 19th IEEE-NPSS Real Time Conference (RT)* (IEEE, 2014) pp. 1–3.
53. "Technical proposal for the SPIRAL2 instrumentation: EXOGAM2" (2009).